ACCEPTED MANUSCRIPT

Orbital selective dynamics in Fe-pnictides triggered by polarized pump pulse excitations

To cite this article before publication: Ganesh Adhikary *et al* 2021 *EPL* in press https://doi.org/10.1209/0295-5075/ac2dc0

epl draft

Orbital selective dynamics in Fe-pnictides triggered by polarized pump pulse excitations

Ganesh Adhikary[1], Tanusree Saha[1], Primož Rebernik Ribič[1,2], Matija Stupar[1], Barbara Ressel[1], Jurij Urbančič[1], Giovanni De Ninno[1,2], A. Thamizhavel[3] and Kalobaran Maiti[3(a)]

[1]*Laboratory of Quantum Optics, University of Nova Gorica, 5001 Nova Gorica, Slovenia.*
[2]*Elettra-Sincrotrone Trieste, Area Science Park, 34149 Trieste, Italy.*
[3]*Department of Condensed Matter Physics and Materials Science, Tata Institute of Fundamental Research, Homi Bhabha Road, Colaba, Mumbai-400005, India*

PACS 74.25.Jb – Electronic structure (photoemission, etc.)
PACS 74.70.Xa – Pnictides and chalcogenides
PACS 78.47.+p – Time-resolved optical spectroscopies and other ultrafast optical measurements in condensed matter
PACS 75.50.Ee – Antiferromagnetics

Abstract. - Quantum materials display exotic behaviours related to the interplay between temperature-driven phase transitions. Here, we study the electron dynamics in one such material, $CaFe_2As_2$, a parent Fe-based superconductor, employing time and angle-resolved photoemission spectroscopy. $CaFe_2As_2$ exhibits concomitant transition to spin density wave state and tetragonal to orthorhombic structure below 170 K. The Fermi surface of this material consists of three hole pockets (α, β and γ) around Γ-point and two electron pockets around X-point. The hole pockets have d_{xy}, d_{yz} and d_{zx} orbital symmetries. The β band constituted by d_{xz}/d_{yz} orbitals exhibit a gap across the magnetic phase transition. We discover that polarized pump pulses can induce excitations of electrons of a selected symmetry. More specifically, while s-polarized light (polarization vector perpendicular to the xz-plane) excites electrons corresponding to all the three hole bands, p-polarized light excites electrons essentially from (α,β) bands which are responsible for magnetic order. Interestingly, within the magnetically ordered phase, the excitation due to the p-polarized pump pulses occur at a time scale of 50 fs, which is significantly faster than the excitation induced by s-polarized light ($\sim$ 200 fs). These results suggest that the relaxation of different ordered phases occurs at different time scales and this method can be used to achieve selective excitations to disentangle complexity in the study of quantum materials.

Introduction. – It is believed that exoticity in quantum materials arises due to complex interplay between spin, charge and orbital degrees of freedom. This makes the research on these materials challenging. A recent addition to this group are the Fe-based compounds [1–3], often exhibiting complex phase diagrams, involving magnetic order, superconductivity and structural transitions [4, 5]. The coexistence of mutually exclusive, magnetic order and superconductivity is one of the many outstanding puzzles observed in these materials, questioning existing theoretical models [6–9]. Numerous investigations allowed scientists to shed light into the fundamental properties of Fe-based systems: the parent compounds exhibit spin density wave (SDW) state at low temperature, accompanied by a structural transition from tetragonal to orthorhombic phase [3,5]. Since multiple bands contribute in the formation of Fermi surfaces, it is difficult to disentangle the role of different orbitals/electronic states in determining the electronic properties of the material.

In order to investigate the possibility of inducing orbital-selective electron dynamics, we studied the polarization-dependent excitation of electrons in an archetypical Fe-based compound $CaFe_2As_2$, a parent Fe-pnictide superconductor. $CaFe_2As_2$ crystallizes in a tetragonal structure at room temperature (space group, $I4/mmm$) with lattice parameters $a = 3.8915$ Å, $c = 11.69$ Å and $z_{As} = 0.372$. At about 170 K [10], it undergoes magnetic transition to the

(a) Corresponding authors: ganesh.adhikary@gmail.com, giovanni.de.ninno@ung.si, kbmaiti@tifr.res.in

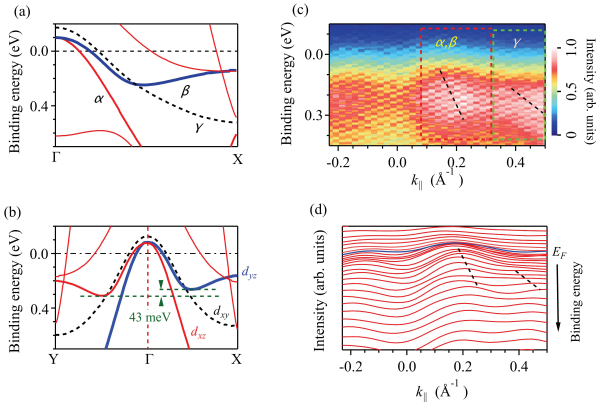

Fig. 1: (color online) Calculated band structure (a) in tetragonal phase along ΓX and (b) in orthorhombic phase along $Y\Gamma X$. In the orthorhombic phase, the degeneracy of d_{xz} and d_{yz} bands is lifted. d_{xy} band also shows different dispersions along ΓX and ΓY. (c) Static ARPES spectrum at 120 K collected using s-polarized higher harmonic laser pulses of energy, 29 eV and the corresponding (d) momentum distribution curves (MDCs). Dashed lines are a guide to the eye.

SDW ground state and structural transition to orthorhombic phase (space group, $Fmmm$; lattice parameters, a = 5.506 Å, b = 5.45 Å, c = 11.664 Å, and z_{As} = 0.36642). Angle resolved photoemission spectroscopy (ARPES) [11] and band structure calculations [12] show that the electronic structure of this material consists of three hole pockets around the Brillouin zone center, Γ and two electron pockets around the zone corner, X (π,π). We have calculated the energy band structure using a full-potential linearized augmented plane wave method as captured in the Wien2k software [13]. The Perdew-Burke-Ernzerhof generalized gradient approximation (GGA) [14] was used for the calculations. In this self-consistent method, the convergence to the ground state was achieved by fixing the energy convergence criteria to 0.0001 Ry (∼1 meV) using 10×10×10 k points within the first Brillouin zone.

The results for the tetragonal structure are shown in Fig. 1(a). Among the three hole bands, the inner two (α/β) bands possess d_{xz}/d_{yz} orbital symmetry. The outer hole band, denoted by γ, has the primary contribution from the d_{xy} orbital. In the SDW phase, the Fe-moments align antiferromagnetically [15] leading to an energy gap in the β band at the Fermi level, E_F [11]. Thus, the magnetic order involves primarily d_{xz}/d_{yz} orbitals. The structural transition often leads to a C_4-symmetry breaking in the Fe-based superconductors at low temperatures [16]. In $CaFe_2As_2$, this leads to a lifting of d_{xz}/d_{yz} degeneracy (energy difference ∼ 43 meV) is observed as shown in Fig. 1(b) [17]. It was reported that the energy bands shift towards higher binding energies upon cooling due to the presence of collapsed tetragonal phase which does not show magnetic order [11]. Evidently, the structural changes will be manifested in the dynamics of all the d-orbitals as observed in Fig. 1(b). Here, we attempted to excite electrons of selected orbital symmetry leaving the other electrons relatively less affected. As discussed in the subsequent sections, we observe that this is possible by exciting the electronic states using light pulses of different polarizations.

Experimental methods. – Time- and angle-resolved photoemission spectroscopy (trARPES) was performed using a mode-locked Ti:sapphire laser [photon energy 1.5 eV (800 nm), pulse duration 40 fs, repetition rate 5 kHz]. The major part of the intensity was used to generate higher-order harmonics spanning the energy range 10-50 eV (pulse duration 40 fs) using Argon medium [18], which is used as a probe pulse. The other part of the beam was used as a pump, whose intensity was controlled with a variable attenuator based on a half wave-plate and a polarizer. We could select the desired harmonics and control their flux by means of a specially-designed grating set-up, which preserves the pulse duration. The photoemission measurements (base pressure $<1\times10^{-10}$ Torr) were performed with an R3000 analyzer and a closed cycle He-cryostat at an energy resolution of 100 meV. Single crystalline $CaFe_2As_2$ samples were grown by the Sn-flux method [19, 20]. The samples were cleaved in-situ to generate a clean and flat surface before every measurement. The dynamics of the photoexcited electrons is studied by varying the time delay between the pump and probe pulses [21, 22].

Results and Discussions. – To start with, we acquired the static (i.e., only probe, no pump) ARPES spectrum of $CaFe_2As_2$ along ΓX-direction. The results obtained at 120 K sample temperature using s-polarized photons of 29 eV are shown in Fig. 1(c). A qualitative comparison can be performed between the experimental spectrum (characterized by an intrinsic low energy resolution due to the use of ultra-short VUV pulses) and the band structure results shown in Figs. 1(a) and 1(b). The experimental spectrum exhibit distinct signatures of the α/β bands separated from the γ band. For better clarity, we show the momentum distribution curves (MDCs) in Fig. 1(d) exhibiting clear representation of the energy bands [11].

After identification of the spectral regimes for various energy bands and the consistency with the reported results, the pump-probe measurements were carried out to study the excited states. We used a probe energy of 20 eV, which corresponds to comparable photoemission cross sections of As 4p and Fe 3d states. This helps emphasizing the changes of these bands having large covalency [23], with good k-resolution. The pump fluence was fixed to 2 mJ/cm^2, which is much below the power required to drive the system into anharmonic regime [24]. In Figs. 2(a) and 2(b), we show the difference of the spectra collected at 200 fs and -300 fs for (a) p-polarized (p-pol) and (b) s-polarized (s-pol) pump excitations (initial sample temperature, 30 K). This provides information on the depleted intensity in the occupied part and enhanced intensity in

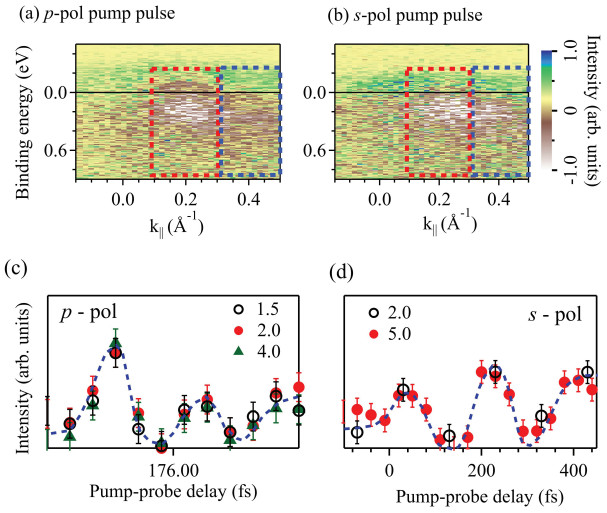

Fig. 2: (color online). The difference spectra for pump-probe time delay, Δt = 200 fs with respect to the data at Δt = -300 fs for (a) p-pol and (b) s-pol pump excitations. Sample temperature is 30 K and the probe pulse energy, $h\nu$ = 20 eV. The red box region corresponds to the (α,β) bands and the blue box region corresponds to the γ band (see Fig. 1(a)). Intensity of hot electrons for (c) p-pol and (d) s-pol pump pulse excitations as a function of pump-probe delay for different pump fluences. Hand drawn smooth lines are a guide to the eye.

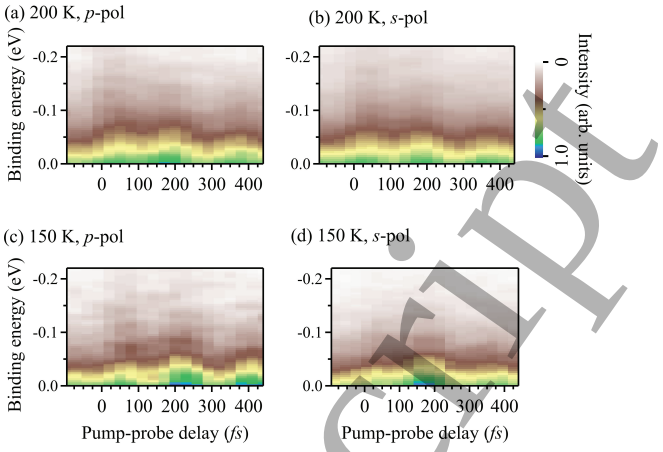

Fig. 3: (color online). Time-resolved spectra (probe energy, $h\nu$ = 20 eV) as a function of pump-probe delay for (a) p-pol and (b) s-pol pump pulses with initial sample temperature of 200 K. The same at an initial sample temperature of 150 K for (c) p-pol and (d) s-pol pump pulses.

the unoccupied part of the electronic structure remaining at 200 fs after the pump-induced excitations; although the pump energy is 1.5 eV, finite population of the unoccupied part close to the Fermi level occurs due to the electron-electron scattering induced relaxations having faster time scale than the time-resolution used in our measurements. The experimental data collected with different polarizations reveal qualitative differences.

In order to investigate, if such a difference can be linked to the fluence of the pump pulse, we have carried out several measurements by varying the fluence of both p-pol and s-pol light. The integrated intensity (momentum integrated for the $k_{||}$ vector along $\Gamma - X$ direction and normalized by the intensity at 50 fs) in the energy range 0.1 - 0.2 eV above the Fermi level as a function of pump-probe delay is shown in Figs. 2(c) and 2(d) for p-pol and s-pol excitations, respectively. The temperature dependent Fermi-Dirac distribution function populates the unoccupied part of the electronic structure just above the Fermi level. Since this effect is significant close to the Fermi level, we have used the energy range of 0.1 - 0.2 eV for our analysis which is far above the energy regime influenced by the Fermi-Dirac distribution function at the temperature range used in our experiments. Therefore, the intensity shown in the figure reflects essentially the population due to the pump-excitations. The experimental results at different pump fluences exhibit identical behavior establishing absence of fluence dependence of the experimental data probed upto 5 mJ/cm^2.

We define the sample surface as xy plane (sample cleaves along c-axis), photoemission occurs in the xz-plane and the detector is placed on the z-axis. In our setup, since the incident beam defines an angle of 36° with z-axis, the electric field vector of p-pol light is closely aligned with the d_{xz} momentum and hence, primarily excites d_{xz} (α, β bands) electrons [22]. The polarization vector of s-pol pulse lies in the xy-plane (along y-axis), which has a finite component along the momentum of d_{xy} and d_{yz} states for excitations. The d_{xz} orbital plane is orthogonal to the polarization direction (y-axis) of the s-pol pulse and hence will be essentially insensitive to s-pol excitations. In the experimental results shown in Fig. 2, it is evident that p-pol pump pulse excites primarily the red box region (α,β bands) as expected from the symmetry selection discussed above, while s-pol light pumps all the three (α,β and γ) bands. This establishes experimentally that the signal corresponding to the p-pol pump excitations, even if k-integrated for the k-vector along $\Gamma - X$ direction, represents the dynamics of (α,β) bands. The s-pol case, on the other hand provides information on the dynamics of all the three bands with the caveat that this is less sensitive to d_{xz} symmetry. We hope these results will help to initiate activities in this direction by some theory group active in the field. In the following part of the manuscript, we analyse the spectral response obtained after k-integration along $\Gamma - X$ direction to achieve good signal to noise ratio quickly without affecting the overall information significantly. This will help to establish applicability of this method without necessitating constrained experimental conditions and avoiding aging effects of the sample surface.

The excited electrons start interacting with each other and the lattice on a time scale of few tens of femtoseconds, leading to different collective excitations involving magnons, phonons, etc. Such optical perturbations may affect the ground state properties. In general, the response related to the electron-phonon coupling is a rel-

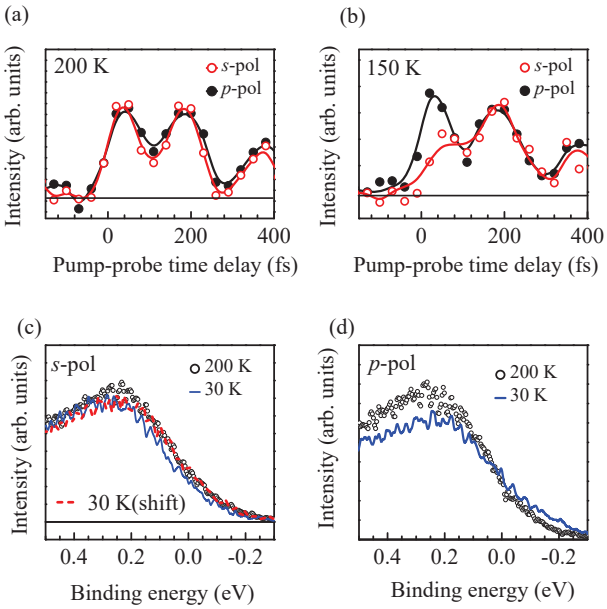

Fig. 4: (color online). The p-pol (closed circles) and s-pol (open circles) intensity of hot electrons at (a) 200 K and (b) 150 K. EDC at Γ-point at a pump-probe delay of 50-fs for the (c) s-polarized and (d) p-polarized pump excitations. Open circles are the data at 200 K and solid line represent 30 K data. The dashed line in (c) is the 30 K data shifted by 35 meV.

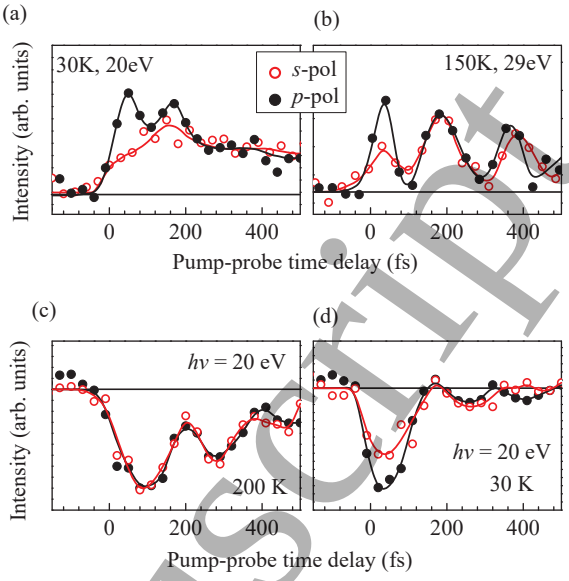

Fig. 5: (color online). (a) Hot electron intensity as a function of pump-probe delay for s-pol (open circles) and p-pol (closed circles) pump excitations with $h\nu = 20$ eV and initial sample temperature of 30 K. (b) The same with $h\nu = 29$ eV and initial sample temperature of 150 K. Time-resolved spectral intensity at 0.2 eV binding energy for p- (solid circles) and s- polarizations (open circles) (probe energy = 20 eV) at (c) 200 K and (d) 30 K.

atively slower process due to the lattice inertia [25], while the electronic phenomena like SDW order will respond relatively fast to the pump-induced excitation [26]. The spectral response of the excited electronic states get modulated by the coherent phonon mode (A_{1g} phonon mode in the present case) [27]. The intensity of the hot electrons for the paramagnetic phase (initial sample temperature = 200 K) are shown in Figs. 3(a), 3(b) and 4(a); the spectral intensities are shown after normalizing the data by the intensities below 1 eV binding energy in order to superimpose them in the same plot. The results exhibit intensity modulation of hot electrons similar for both p-pol and s-pol pump excitations. In the SDW phase (initial sample temperature = 150 K), when the system is excited with p-pol light, the maximum yield of intensity occurs at ∼50 fs, as shown in Figs. 3(c) and 4(b). However, a maximum is observed at about ∼170 fs for the pumping with s-pol light as shown in Figs. 3(d) and 4(b).

In order to understand the scenario, we analyze the energy distribution curve (EDC) at Γ-point ($\Delta k = 0.0 \pm 0.035$ Å^{-1}) collected at a pump-probe delay of 50 fs; the data are normalized by the intensity below 1 eV binding energy, which does not show significant change in intensity due to the pump excitations. It is evident from Fig. 4(c) that for the s-pol pump excitations, the leading-edge midpoint (LEM) at 30 K is shifted by 35 meV below the LEM of the spectra at 200 K suggesting survival of the SDW gap. Interestingly, the p-pol case shown in Fig. 4(d) exhibits LEM at the same energy at 200 K and 30 K data revealing evidence of the melting of SDW order. These results demonstrate the survival of the SDW order in the s-pol case while the SDW phase is melted in the p-pol case; the time scale of the melting of the SDW order is manifested by an intense peak at 50 fs delay in the p-pol case shown in Fig. 4(b).

The electron yield above E_F can be associated, via the Fermi-Dirac distribution function, to the increase of the transient electronic temperature, T_e, which is responsible for the melting of the magnetic and structural long-range order [28]. Thus, a peak at 50 fs time delay for the p-pol excitation case and its virtual absence for the s-pol case (intensity at 50 fs is negligibly small with the peak appearing at 170 fs) reveal an interesting scenario: the changes in magnetic and structural orders may be triggered on different time scales. An earlier study [29] suggested nematic processes in Fe-based materials to happen instantaneously after excitation within the time resolution (170 fs for pump pulse and 250 fs for probe pulse) used in those measurements. Employment of 40 fs time resolution reveals the difference between the time-scales for the melting of magnetic and structural order. While this conclusion has interesting implication in the study of electronic properties of complex quantum materials, this also suggests that one can reveal orbital selective dynamics using polarized pump pulse excitations.

In order to further support the above scenario, we carried out some additional experiments. In Fig. 5(a), we show the trARPES spectra at 30 K for p- and s-polarizations of pump pulses with photon energy 20 eV;

the data show the photoelectron yield. We observe that the photoelectron intensity rises very fast when the system is excited with p-pol light. When the system is excited with s-pol light, the yield of intensity rises slowly and the maximum intensity appears at a delay time of $\sim$ 200 fs.

In order to verify the transient dynamics at another k-point, we used probe photon energy of 29 eV, which is close to the Γ-point on the k_z-axis, ($k_z \approx 12\pi/c$) at an initial sample temperature of 150 K. Since the relative photoemission cross-section of As 4p states gets suppressed at this energy, Fe 3d contributions will be dominant in the spectral intensity. Once again, the experimental results shown in Fig. 5(b) exhibit a maximum yield of intensity at $\sim$50 fs when the system is excited with p-pol light, while the yield of intensity is maximum at about $\sim$200 fs when the system is excited with s-pol light.

ARPES results [11] exhibit back folding of the β-band occurring around 0.2 Å^{-1} below 170 K due to the SDW order, which extends till Γ-point. In Fig. 5(c) and (d), we plot the k-integrated spectral intensity at the binding energy of 0.2 eV, which, below the critical temperature (e.g. at 30 K), reflects the yield of the folded band due to SDW order; probe pulse energy is 20 eV. Above threshold (200 K), we do not observe discernible difference between the p-pol and s-pol case, see Fig. 5(c). However, at 30 K, we observe significantly more intense dip in p-pol case compared to the s-pol case shown in Fig. 5(d). This confirms that the folded band formed due to the SDW order is more efficiently depopulated in the p-pol case. Note that the relaxation of the hole states at 30 K is much faster compared to 200 K, which is in agreement with the other measurements [27].

Above the magnetic ordering temperature, the α and β bands have both d_{xz} and d_{yz} characters as the crystal structure is tetragonal. Therefore both p- and s-polarized pumps are able to excite them; the difference in intensity of excitations might be related to the cross section due to the component of light polarization vector along the orbital lobes. In the magnetically ordered phase, the structure becomes orthorhombic and the degeneracy of d_{xz} and d_{yz} electrons is lifted. Evidently, the p-polarized light is able to excite d_{xz} electrons which are coupled via electron-magnon coupling and the response occurs at a fast time scale. On the other hand, s-polarized light is not able to excite the electrons participating in the magnetic order and the slower electron temperature rise might be related to the relatively slower electron-phonon response.

It is to note here that L. Rettig *et al.* [27] have studied the perturbation dynamics for optically excited $EuFe_2As_2$ to investigate different coupling phenomena and reported different time scales for magnetic ordering ($\sim$50 fs) and structural orientation ($\sim$100 fs). While our results are consistent with those findings, we discover that electrons corresponding to different symmetry can be selectively excited by using suitably polarized pump pulses. The difference in the reported study is the use of a polarized pump pulse, instead of a polarized probe pulse, as it was used in earlier studies [30]. Since the electron-phonon coupling mixes up the symmetries of the excited intermediate states, the polarized probe pulse cannot distinguish the orbital-selective ground state properties [22]. On the other hand, excitation with an ultrafast pump pulse allows one to disentangle symmetries associated to varied excitations. This implies that a pump pulse may in principle excite electrons of selective symmetry without affecting electrons of the other symmetry. While this description explains the experimental results qualitatively, we hope that these results will trigger theoretical activities in this direction.

These results also indicate that the magnetic and structural orders may not be linked. This explains various observations of structural and magnetic orders occurring at two different temperatures. For example, Co doping in $Ba(Fe_{1-x}Co_x)_2As_2$ show that the structural transition precedes the magnetic transition [31]. On the other hand, with the application of external pressure on $BaFe_2As_2$, the magnetic transition precedes the structural one [32].

Conclusions. – In summary, we studied the electron dynamics in a parent compound in the Fe-pnictide superconductor family using time-resolved angle-resolved photoemission spectroscopy. Our results suggest that light polarization of the pump pulse in a pump-probe measurement can be exploited to study orbital selective excitation dynamics in complex quantum materials. Employing this method, we show that the excitation dynamics due to the s-polarized pump pulse excitation of the electronic states near the Fermi level in $CaFe_2As_2$ is relatively slower ($\sim$ 200 fs) than the dynamics of electrons probed by p-polarized pump pulse excitations ($\sim$ 50 fs). Clearly, the electronic properties linked to the corresponding orbital symmetries are occurring at different time scales. This is in line with the discoveries of orbital selective behavior such as β-bands show an emergence of a band gap across SDW transition while the Fermi surfaces corresponding to other bands survive [11], orbital selective Mottness [33], etc. These results show an experimental method to probe such orbital selective behavior which has significant implication in the study of underlying physics of complex quantum materials.

Acknowledgements. – KM acknowledges the financial support from the Department of Atomic Energy, Government of India under the DAE-SRC-OI Award program (Grant no. 21/08/2015-BRNS/35075). This work has received funding from the European Unions Horizon 2020 research and innovation programme under the Grant Agreement No. 654360 NFFA-Europe. We also acknowledge the support of the FLAG-ERA JTC 2019 project DIMAG.

REFERENCES

[1] Kamihara, Y. et al., *J. Am. Chem. Soc.*, **128** (2006) 10012.

[2] Kamihara, Y., Watanabe, T., Hirano, M. and Hosono, H. , *J. Am. Chem. Soc.*, **130** (2008) 3296.

[3] Ishida, K., Nakai, Y. and Hosono, H. , *J. Phys. Soc. Jpn.*, **78** (2009) 062001; Maiti, K., *Pramana - J. Phys.*, **84** (2015) 947.

[4] Stewart, G. R., *Rev. Mod. Phys.*, **83** (2011) 1589.

[5] Sobota, J. A., He, Y. and Shen, Z. X., *Rev. Mod. Phys.*, **93** (2021) 025006.

[6] Kurita, N. et al., *Phys. Rev. B*, **83** (2011) 214513; Adhikary, G., *J. Phys. Condens. Matter*, **25** (2013) 225701.

[7] Dai, P., Hu, J., and Dagotto, E. , *Nat. Phys.*, **8** (2012) 709.

[8] Chubukov, Andrey and Hirschfeld, Peter J., *Physics Today*, **68** (2015) 46.

[9] Hirschfeld, Peter J., *Comptes Rendus Physique*, **17** (2016) 197.

[10] Soh, J. H. et al., *Phys. Rev. Lett.*, **111** (2013) 227002.

[11] Ali, K. et al., *Phys. Rev. B*, **97** (2018) 054505; Adhikary, G. et al., *J. Appl. Phys.*, **115** (2014) 123901.

[12] Ali, K. and Maiti, K. , *Sci. Rep.*, **7** (2017) 6298.

[13] Blaha, P., Schwarz, K., Madsen, G. K. H., Kvasnicka, D. and Luitz, J. , *WIEN2k: An Augmented Plane Wave Plus Local Orbitals Program for Calculating Crystal Properties (Karlheinz Schwarz, Technische Universität Wien, Austria)*, (2001)

[14] Perdew, J. P., Burke, K. and Ernzerhof, M. , *Phys. Rev. Lett*, **77** (1996) 3865.

[15] Goldman, A. I. et al., *Phys. Rev. B*, **78** (2008) 100506(R).

[16] Fernandes, R. M., Chubukov, A. V. and Schmalian, J., *Nat. Phys.*, **10** (2014) 97; Pfau, H. et al., *Phys. Rev. Lett.*, **123** (2019) 066402; Yang, Y. et al., *Nat. Phys.*, **16** (2020) 514.

[17] Ming, Y. et al., *Proc. Natl. Acad. Sci. U.S.A.*, **108** (2011) 6878; Ali, K. and Maiti, K. , *Eur. Phys. J. B*, **91** (2018) 199.

[18] Grazioli, C. et al., *Rev. Sci. Instrum.*, **85** (2014) 023104.

[19] Kumar, N. et al., *Phys. Rev. B*, **79** (2009) 012504.

[20] Mittal, R. et al., *Phys. Rev. Lett*, **102** (2009) 217001.

[21] Brorson, S. D. et al., *Phys. Rev. Lett.*, **64** (1990) 2172.

[22] Adhikary, G. et al., *Phys. Rev. B*, **98** (2018) 205142.

[23] Adhikary, G. et al., *J. Appl. Phys.*, **114** (2013) 163906.

[24] Mansart, B. et al., *Phys. Rev. B*, **80** (2009) 172504.

[25] Schmitt, F. et al., *Science*, **321** (2008) 1649.

[26] Petersen, J. C. et al., *Phys. Rev. Lett.*, **107** (2011) 177402.

[27] Rettig, L. et al., *Phys. Rev. Lett.*, **108** (2012) 097002.

[28] Nicholson, C. W. et al., *Phys. Rev. Lett.*, **117** (2016) 136801.

[29] Shimojima, T. et al., *Nat. Commun.*, **10** (2019) 1946.

[30] Yang, L.X. et al., *Phys. Rev. Lett.*, **112** (2014) 207001.

[31] Nandi, S. et al., *Phys. Rev. Lett.*, **104** (2010) 057006.

[32] Wu, J. J. et al., *Proc. Natl. Acad. Sci. U.S.A.*, **110** (2013) 17263.

[33] Medici, L. de, Giovannetti, G. and Capone, M., *Phys. Rev. Lett.*, **112** (2014) 177001.